



HAL
open science

A model of the within-population variability of budburst in forest trees

Jianhong Lin, Daniel Berveiller, Christophe François, Heikki Hänninen,
Alexandre Morfin, Gaëlle Vincent, Rui Zhang, Cyrille Rathgeber, Nicolas
Delpierre

► **To cite this version:**

Jianhong Lin, Daniel Berveiller, Christophe François, Heikki Hänninen, Alexandre Morfin, et al.. A model of the within-population variability of budburst in forest trees. *EGUsphere*, In press, pp.1-25. 10.5194/egusphere-2023-1075 . hal-04294652

HAL Id: hal-04294652

<https://hal.science/hal-04294652>

Submitted on 20 Nov 2023

HAL is a multi-disciplinary open access archive for the deposit and dissemination of scientific research documents, whether they are published or not. The documents may come from teaching and research institutions in France or abroad, or from public or private research centers.

L'archive ouverte pluridisciplinaire **HAL**, est destinée au dépôt et à la diffusion de documents scientifiques de niveau recherche, publiés ou non, émanant des établissements d'enseignement et de recherche français ou étrangers, des laboratoires publics ou privés.



Distributed under a Creative Commons Attribution 4.0 International License



1 A model of the within-population variability of budburst in forest 2 trees

3

4 Jianhong Lin^{1,*}, Daniel Berveiller¹, Christophe François¹, Heikki Hänninen^{2,3}, Alexandre Morfin¹,
5 Gaëlle Vincent¹, Rui Zhang^{2,3}, Cyrille Rathgeber⁴, Nicolas Delpierre^{1,5,*}

6 ¹ Université Paris-Saclay, CNRS, AgroParisTech, Ecologie Systématique et Evolution, 91190, Gif-sur-Yvette, France.

7 ² State Key Laboratory of Subtropical Silviculture, Zhejiang A&F University, Hangzhou, China

8 ³ SFGA Research Center for *Torreya grandis*, Zhejiang A&F University, Hangzhou, China

9 ⁴ INRAE, SILVA, Université de Lorraine, AgroParisTech, Nancy, France

10 ⁵ Institut Universitaire de France (IUF)

11 * Correspondence to: jianhong.lin@universite-paris-saclay.fr, nicolas.delpierre@universite-paris-saclay.fr

12 **Abstract.** Spring phenology is a key indicator of temperate and boreal ecosystems' response to climate change. To
13 date, most phenological studies have analyzed the mean date of budburst in tree populations while overlooking the
14 large variability of budburst among individual trees. The consequences of neglecting the within-population variability
15 (WPV) of budburst when projecting the dynamics of tree communities are unknown. Here, we develop the first model
16 designed to simulate the WPV of budburst in tree populations. We calibrated and evaluated the model on 48,442
17 budburst observations collected between 2000 and 2022 in three major temperate deciduous trees, namely, hornbeam
18 (*Carpinus betulus*), oak (*Quercus petraea*) and chestnut (*Castanea sativa*). The WPV model received support for all
19 three species, with a root mean square error of 5.6 ± 0.3 days. Retrospective simulations over 1961-2022 indicated
20 earlier budburst as a consequence of ongoing climate warming. However, simulations revealed no significant change
21 for the duration of budburst (DurBB, i.e., the time interval from BP20 to BP80, which respectively represent the date
22 when 20% and 80% of trees in a population have reached budburst), due to a lack of significant temperature increase
23 during DurBB in the past. This work can serve as a basis for the development of models targeting intra-population
24 variability of other functional traits, which is of increasing interest in the context of climate change.

25 Keywords: budburst variability; model; temperate trees; climate warming; budburst duration; population.

26 1. Introduction

27 Phenology, as the study of recurrent biological events such as budburst in spring, has attracted increasing attention due
28 to climate warming (Piao et al., 2019). The timing of leaf phenology in spring is a major indicator of climate warming
29 (Parmesan and Yohe, 2003) and is mainly modulated by temperature (Menzel et al., 2006; Zhang et al., 2022; Zhang
30 et al., 2021; Chen et al., 2018; Vitasse et al., 2009a) and photoperiod (Delpierre et al., 2016; Fu et al., 2019; Vitasse
31 and Basler, 2013; Meng et al., 2021). In the northern hemisphere, it is well established that spring phenological events
32 have been advanced by climate warming (Walther et al., 2002; Menzel et al., 2006), although this advancement is
33 currently slowing down (Fu et al., 2015; Chen et al., 2019). To date, massive efforts have been made to study the
34 spatiotemporal variability of leaf phenology among tree populations and across years (Delpierre et al., 2016; Fu et al.,
35 2015; Meng et al., 2021; Chen et al., 2018). However, the variability of leaf phenology within populations has received



36 little attention to date (Scotti et al., 2016; Delpierre et al., 2017), which is in line with the general focus of ecological
37 studies on average traits (Violle et al., 2012). This is intriguing, since the within-population (i.e., tree-to-tree) variability
38 of phenological events is vast and can even be equivalent to that observed among populations (Delpierre et al., 2017;
39 Vitasse et al., 2009a; Rathgeber et al., 2011). It typically takes 1 to 4 weeks from the first to the last tree to burst buds
40 in a population (Denechere et al., 2021), with an average of 19 days (Delpierre et al., 2017). Furthermore, the duration
41 from the first to last tree to burst buds in a given population varies annually (Denechere et al., 2021).

42 The large within-population variability (WPV) of budburst observed in natural tree populations is considered to result
43 from their exposure to a large range of fluctuating environmental (e.g., frost) and biotic (e.g., herbivores and pathogens)
44 selection pressures, which alternatively favor trees that burst buds early or late (Alberto et al., 2011). From an
45 evolutionary point of view, this phenotypic diversity has an adaptive value at the population scale, because the
46 environment is likely to change across the lifetime of trees (Petit and Hampe, 2006; Morente-Lopez et al., 2022;
47 Blanquart et al., 2013). For instance, if a local climate becomes suitable in early spring under climate warming, trees
48 that burst buds early will benefit from an extended growing season, thus maximizing their carbon assimilation and
49 possibly their biomass production (Zohner et al., 2020; Delpierre et al., 2009; Richardson et al., 2010), which will
50 allow them to gradually occupy a dominant position in the population. Moreover, early budburst enables trees to escape
51 pathogens (e.g., for oak, see Dantec et al., 2015). On the contrary, if freezing events occur frequently in early spring
52 with the advance of budburst, late trees can grow better by avoiding freezing injury (Delpierre et al., 2017; Zohner et
53 al., 2020; Puchalka et al., 2016). Moreover, the WPV also affects interactions with competing plants and herbivores
54 (Hart et al., 2016; Renner and Zohner, 2018).

55 The WPV of budburst is probably underpinned by genetic diversity, as evidenced by the variability of phenological
56 traits among individual trees that experience similar environmental conditions (Bontemps et al., 2016; Delpierre et al.,
57 2017). This genetic determinism is further reflected in the year-to-year repeatability of the phenological ranking of
58 individuals within tree populations (Delpierre et al., 2017). In addition to this genetic determinism, the WPV is also
59 likely influenced by micro-environmental variations such as the unbalanced distribution of soil-water content within
60 populations, edaphic conditions, or microtopography (Delpierre et al., 2017; Denechere et al., 2021; Scotti et al., 2016).

61 To the best of our knowledge, the question of whether and to what extent would the WPV of budburst be modified in
62 the current context of climate change has not been addressed so far. Quantifying WPV as the duration (in days) from
63 the first to the last tree to burst buds in one population, we identify three alternative hypotheses for the modification
64 of WPV with climate change: (i) the duration of budburst remains unchanged because all trees in the population
65 advance to the same extent; (ii) the duration of budburst decreases because of the increasing warming rate during the
66 budburst period (Malyshev et al., 2022); (iii) the duration of budburst increases because of insufficient chilling
67 accumulation, as hypothesized previously from experimental studies (Zohner et al., 2018; Zhang et al., 2021).

68 Phenological research has made extensive use of modeling to study the response of the spatiotemporal variability of
69 budburst to climate warming (Zhang et al., 2022; Meng et al., 2021; Delpierre et al., 2009; Chuine and Regnier, 2017).
70 The models postulate that temperature and photoperiod are the main environmental cues that trigger budburst in boreal
71 and temperate (Delpierre et al., 2009; Kramer, 1994; Hänninen and Kramer, 2007), subtropical (Zhang et al., 2022; Du



72 et al., 2019), and tropical trees (Chen et al., 2017). In these models, temperature plays a dual role. Endodormancy is
73 released by chilling in late autumn or winter, with high temperatures allowing for ontogenetic growth during the
74 ecodormancy stage (Hänninen, 2016; Jewaria et al., 2021). Meanwhile, there is an interaction between these two stages
75 in the models, namely, ontogenetic growth is influenced by dormancy release (Hänninen, 2016; Hänninen and Kramer,
76 2007; Vegis, 1964). Lundell et al. (2020) further proved that this interaction can be affected by prevailing temperatures.
77 One important point is that these models do not pay attention to the WPV of phenological traits. They have been
78 parameterized and applied to predict the mean or median date of budburst in a given tree population (Lundell et al.,
79 2020; Kramer, 1994; Zhang et al., 2022). In other words, these models simulate the timing of budburst as a discrete
80 event in the population without considering the WPV of leaf phenology. To the best of our knowledge, only two studies
81 to date, notably (Rousi and Heinonen, 2007) in Birch (*Betula pendula*) and (Langvall et al., 2001) in Norway spruce
82 (*Picea abies* (L.) Karst.), have attempted to establish a link between WPV and environmental conditions through the
83 temperature sum required for the opening of buds at the scale of individual trees. At the scale of tree populations, a
84 distribution of temperature sums to budburst was also used in the so-called physio-demo-genetic (PDG) models
85 (Kramer et al., 2008; Oddou-Muratorio and Davi, 2014) to simulate the adaptive potential of tree populations. However,
86 a systematic model for the WPV of budburst is still lacking.

87 Here we developed a model that simulates the WPV of budburst in temperate deciduous trees. We calibrated and
88 validated the model over an extensive budburst dataset acquired from five tree populations at the individual tree scale
89 over 23 years (representing 48,442 observations). Specially, we aim to 1) develop the WPV model and validate its
90 ability for predicting the progress of budburst in tree populations, 2) use the model to in a retrospective simulation
91 exercise testing whether the duration of budburst period in the population changed with climate warming in the recent
92 decades.

93 **2. Materials and Methods**

94 **2.1 Study sites**

95 We used budburst data collected from two forests located near Paris (France): Barbeau (48.476° N, 2.780° E, 95 m asl)
96 and Orsay (48.705° N, 2.167° E, 105 m asl). At these sites, the progress of budburst was observed at the individual
97 scale in populations of three major temperate deciduous tree species, namely, hornbeam (*Carpinus betulus* L.), oak
98 (*Quercus petraea* (Matt.) Liebl) and chestnut (*Castanea sativa* Mill.). Hornbeam is an early leafing tree species,
99 chestnut is a late species while oak is intermediate. Hornbeam and oak are present in both forests, while chestnut is
100 present in Orsay only (Table 1). For each species, we focused on healthy and dominant trees, except for hornbeam (an
101 understory species). We collected budburst observations from 2000 to 2022, which yielded a dataset comprising 5
102 populations and 103 population-years. In each population, we observed between 28 and 309 individuals (mean 90)
103 (Table 1).

104

105



106 **Table 1. Description of the phenological and meteorological datasets.**

Phenology Site	Coordinate	Meteorological station	Coordinate	Species	Number of year	Number of data	Number of trees (min / max / average)	Observation years
Orsay	48.705° N, 2.165° E	Gometz-le- Châtel	48.677° N, 2.136° E	<i>Quercus</i>	23	153	29/190/85	2000-2022
				<i>Carpinus</i>	20	124	29/146/50	2002-2006, 2008- 2022
				<i>Castanea</i>	21	112	29/192/80	2000-2007, 2010- 2022
Barbeau	48.476° N, 2.780° E	Châtelet-en- Brie	48.491° N, 2.802° E	<i>Quercus</i>	20	87	29/309/154	2003-2022
				<i>Carpinus</i>	19	64	28/241/114	2004-2022

107

108 **2.2 Phenology dataset**

109 A team of eight local observers (including most of the authors of this paper) conducted the observations of developing
 110 buds in the tree crowns throughout spring. The observers used binoculars and occasionally received training in order
 111 to reduce observer bias (Liu et al., 2021). The interval between phenological observations was of 4 days on average
 112 (from 2 to 7 days). A tree was considered to have burst its buds when at least 50% of the buds in the upper third of the
 113 crown presented leaves that extended beyond the tip of the scales, which corresponded to stage BBCH 9 (Meier, 1997).
 114 At each observation date, we calculated the percentage of trees that had reached budburst in the tree population,
 115 dividing the number of trees at BBCH 9 by the total number of trees observed on that date and multiplying the result
 116 by 100.

117 **2.3 Temperature data**

118 We obtained the mean daily temperature data from the meteorological station nearest to the study sites (Table 1).
 119 However, there were missing values in the temperature data collected from the stations, especially before 1970. To fill
 120 these gaps and predict the missing data in order simulate budburst in previous years, we used the SAFRAN reanalysis
 121 data (grid-resolution of 8*8 km²) (Vidal et al., 2010), which we de-biased by establishing a linear regression between
 122 the local and corresponding SAFRAN temperature data from September of previous year to June.

123 **2.4 Model description**

124 We introduce a novel model, named the within-population variability (WPV) model, which was constructed to predict
 125 the progress of budburst in tree populations (i.e., percentage of trees having burst buds at a given date in a tree
 126 population). We hypothesized that the difference between individuals in the population was reflected in the difference
 127 of the forcing accumulation requirement (F^*).

128 We built the WPV model by modifying a state-of-the-art process-based model that simulated a discrete budburst event
 129 (i.e., budburst of an individual plant or mean budburst date in a tree population) (Lundell et al., 2020). In short, the
 130 model represents the release of endodormancy through the accumulation of “chilling” temperatures and simulates the
 131 ontogenetic growth of buds through the accumulation of “forcing” temperatures. One particularity of the model is that
 132 ontogenetic growth is regulated by the state of rest break and the prevailing temperature (Lundell et al., 2020; Hänninen,
 133 1990; Hänninen and Kramer, 2007; Vegis, 1964). The ontogenetic competence, Co (a dimensionless [0, 1] multiplier),



134 is applied to represent this regulation (Lundell et al., 2020; Hänninen and Kramer, 2007; Hänninen, 2016). In the model,
135 budburst is considered to occur at date t when a given sum of the forcing temperature is reached such that $F(t) \geq F^*$.
136 In the WPV model, we assumed that F^* followed a normal distribution at the level of the tree population (see Fig. S1
137 for a flow chart of the model). At each date t , the model simulates the proportion of the population (BP, for *budburst*
138 *percent*) that has fulfilled the forcing accumulation requirement:

$$139 \quad F^* = (\mu, \sigma^2) \quad \text{eq.1}$$

$$140 \quad BP(t) = 0.5 \times (1 + \operatorname{erf}(\frac{F(t)-\mu}{\sigma \times \sqrt{2}})) \times 100 \quad \text{eq.2}$$

141

142 Where $F(t)$ is the forcing degree-day accumulation reached on day t , μ is the mean of normal distribution, σ is the
143 standard deviation of normal distribution, and erf is the Gaussian error function.

144

145 The forcing accumulation $F(t)$ is calculated as the integral of a “forcing rate” as follows:

$$146 \quad F(t) = \sum_{d=270}^t Rf_{act} \quad \text{eq.3}$$

147 Where d is the start date of forcing accumulation ($d = \text{DoY } 270$ in the previous year). In this model, the stage of
148 dormancy release and the stage of ontogenetic growth can occur simultaneously (i.e., the model belongs to the “parallel”
149 model category) (Hänninen, 2016; Chuine and Regnier, 2017). However, the forcing rate Rf_{act} , which is the actual
150 rate of ontogenetic growth, is affected by both temperatures and ontogenetic competence (Co). It is calculated as
151 follows:

$$152 \quad Rf_{act}(t) = Rf(t) * Co(t) \quad \text{eq. 4}$$

153 Where $Rf(t)$ is the potential rate of ontogenetic growth at time t , and Co is the ontogenetic competence at time t ; these
154 two variables are calculated as follows:

$$155 \quad Rf(t) = \begin{cases} 0, & T(t) < T_b \\ T(t) - T_b, & T(t) \geq T_b \end{cases} \quad \text{eq. 5}$$

156 Where T_b is the temperature threshold ($^{\circ}\text{C}$) above which forcing accumulation occurs.

157 The ontogenetic competence Co varies over time and is simulated as:

$$158 \quad Co(t) = \max(0; \min(1; g \times T(t) + h + \frac{Sr(t)}{100} * (1 - h))) \quad \text{eq.6}$$

159 Where $Co(t)$ is the ontogenetic competence at time t in the range $[0, 1]$, which modulates the effect of the state of rest
160 break on the rate of ontogenetic growth (see Fig. S2). When $Co=0$, ontogenetic growth is stopped. The ability of
161 ontogenetic growth is restored between $Co=0$ and $Co=1$ with rest breaking. Finally, g and h are parameters (Lundell
162 et al., 2020), $T(t)$ is the daily mean temperature, and $Sr(t)$ is the state of rest break at time t , which is calculated as
163 follows:



164
$$Sr(t) = C_{tot}/C_{cri} \quad \text{eq.7}$$

165 Where C_{cri} is the chilling requirement for rest completion, and C_{tot} is the actual accumulation of chilling temperature,
 166 quantified as the number of chilling units (in chill units C.U.) and calculated from DoY=270 of the previous year up
 167 to time t as follows:

168
$$C_{tot} = \sum_{d=270}^t Rc \quad \text{eq.8}$$

169 Where the daily rate of chilling accumulation (Rc) is calculated as follows:

170
$$Rc = \begin{cases} 1, & T(t) < T_c \\ 0, & T(t) \geq T_c \end{cases} \quad \text{eq.9}$$

171 Where T_c is the temperature threshold (°C) below which chilling accumulation occurs.

172 **2.5 Parameter estimation**

173 We calibrated the model using budburst data obtained during the period 2000-2016 in Orsay (all three species:
 174 hornbeam, oak, chestnut) and then validated it using data from 2017-2022 in Orsay (three species) and from 2000-
 175 2022 in Barbeau (two species: hornbeam and oak). The model was therefore calibrated over 17 years for the three
 176 species (Orsay populations, representing 52, 71 and 50 observation dates for hornbeam, oak and chestnut, respectively)
 177 and validated over 29 site-years for hornbeam and oak (representing 89 and 114 observation dates, resp.), and 6 years
 178 (29 observation dates) for chestnut. A previous study (Vitasse et al., 2009b) provided evidence of similar apparent
 179 phenological responses to temperature among populations of the same species located as far as 650 km apart, which
 180 also suggests the low differentiation of phenological traits across populations. Orsay and Barbeau populations are
 181 separated by a distance of 50 km and experience a similar climate. This is why we used the Barbeau data as a validation
 182 counterpart to the Orsay data used for calibration. The model predicts the percentage of budburst in the population
 183 (from 0% to 100% budburst) along with the corresponding date. Thus, we calculated the root mean square error (RMSE)
 184 over two dimensions (Fig. S3). First, we calculated RMSE over the percentage of budburst in the tree population (i.e.,
 185 comparing the difference between the observed and predicted budburst percent occurring on the same day of the year,
 186 DoY).

187
$$RMSE_{BP} = \sqrt{\frac{\sum_{i=1}^n (\sqrt{num} \times (BP_{obs,i} - BP_{pred,i})^2)}{\sum_{i=1}^n \sqrt{num}}} \quad \text{eq.10}$$

188 Where $RMSE_{BP}$ is the root mean square error for budburst percent (expressed in percent), num is the number of trees
 189 observed on a given day of the year, $BP_{obs,i}$ is the observed percentage of budburst of datum i , $BP_{pred,i}$ is the predicted
 190 percentage of budburst of same datum, and n is the total number of data (e.g., $n=50$ in a hypothetical case where the
 191 percentage of budburst has been observed five times per year on average over 10 years in a given population). We used
 192 \sqrt{num} as a weight in the calculation of squared errors to compensate for the fact that a very large number of trees
 193 (i.e., >300 trees) were observed at some dates: these observations are more representative of the actual percentage of
 194 budburst in the population (as compared to observations established for a smaller number of trees), although they also
 195 tend to overrepresent them in the calculation of errors.



196 We then calculated the RMSE of dates (i.e., comparing the difference, in number of days, between the observations
197 and predictions for the same percentage of budburst; Fig. S3).

$$198 \quad RMSE_{DoY} = \sqrt{\frac{\sum_{i=1}^n (\sqrt{num} \times (DoY_{obs,i} - DoY_{pred,i}))^2}{\sum_{i=1}^n \sqrt{num}}} \quad \text{eq.11}$$

199 Where $RMSE_{DoY}$ is the root mean square error for the budburst date (in days), num is the number of trees observed,
200 $DoY_{obs,i}$ is the observed date of budburst of datum i (e.g., the date when we observed 24% budburst for the population
201 of interest in a given year), $DoY_{pred,i}$ is the predicted date of budburst of the same datum (e.g., the date when the model
202 predicted 24% budburst in the same tree population and year), and n is the total number of data.

203 Finally, we calculated the total RMSE as follows:

$$204 \quad RMSE_{tot} = RMSE_{BP} + RMSE_{DoY} \quad \text{eq.12}$$

205 In the calibration stage, we determined the best parameter set as the one that minimized $RMSE_{tot}$.

206 In addition to RMSE, we also used mean bias error to evaluate the model forecast accuracy (in terms of budburst
207 percentage or DoY), which is calculated as follows:

$$208 \quad \text{mean bias} = \frac{1}{N} \sum_{i=1}^N (obs_i - pred_i)$$

209 Where obs_i and $pred_i$ are the i -th observation and prediction, respectively, N is the number of observations.

210 **2.6 Evaluating the modelled F^* distributions**

211 To validate the modelled F^* distribution, we simulated the distribution of the forcing accumulation at the date of each
212 BP observation. Because there are different observed BP in each year. We binned the observed BP data into 11 groups
213 (i.e., BP0, BP10, BP20...BP100, e.g., we regard the data between BP5 (date at which 5% trees burst buds) to BP15
214 (date at which 15% trees burst buds) as group “BP10”; note that BP0 refers to dates at which 5% or less trees have
215 burst buds, and BP100 refers to dates at which 95% or more trees have burst buds). Then we used a sigmoid function
216 to simulate the relation between BP and averaged corresponding forcing accumulation across all the years. We also
217 calculated their first derivatives (i.e., the increasing of BP per unit of forcing accumulation). Moreover, we calculated
218 the distribution of observed BP across all the years.

219 **2.7 Evaluating the response of the within-population variability of budburst to climate warming**

220 We used our model to predict budburst in the past (1961-2022) using historical daily mean temperature data and gap-
221 filled data using debiased SAFRAN reanalysis of temperatures (see above).

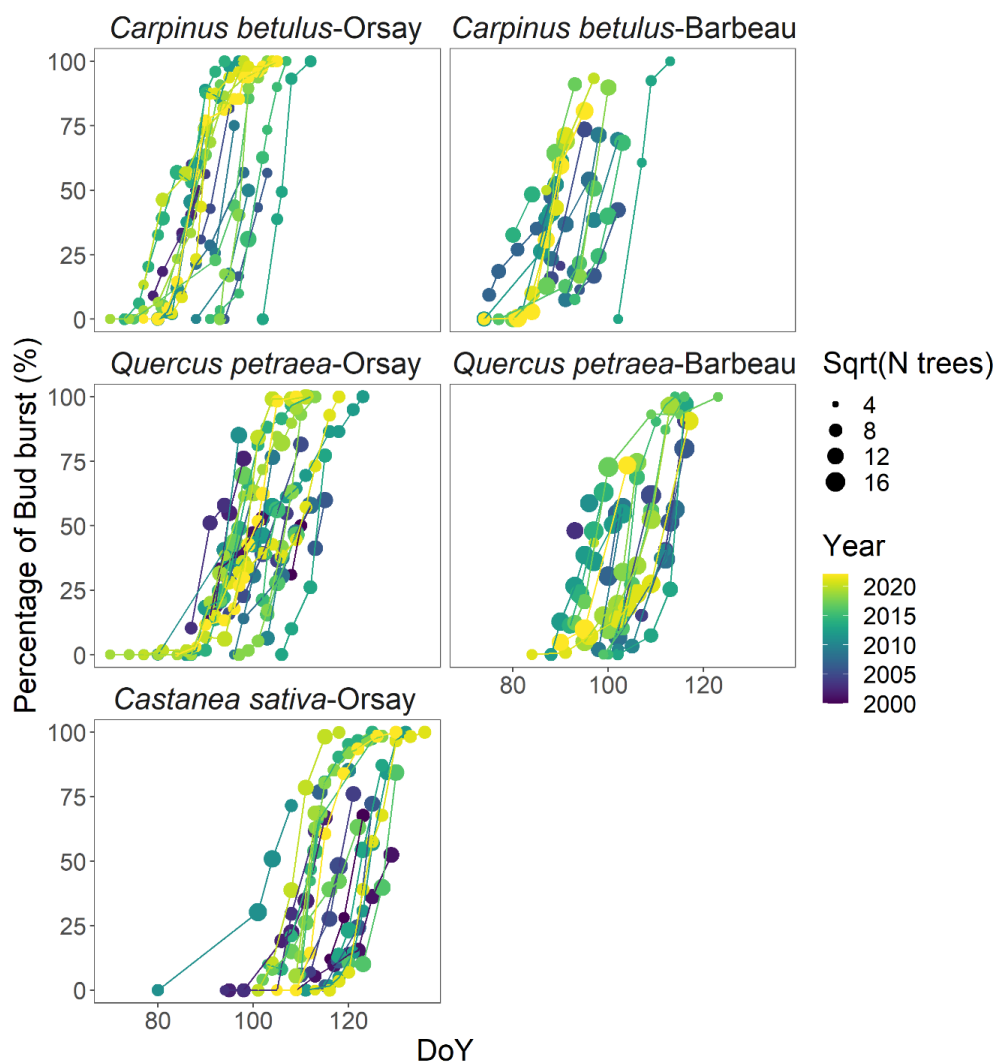
222 As explained earlier, our model simulates the percentage of budburst in a tree population at a given date. To evaluate
223 the response of the WPV of budburst to climate warming, we focused on the particular dates at which 20% and 80%
224 of trees in a given population had reached budburst (termed BP20 and BP80, respectively) and the duration between
225 these two dates (DurBB = BP80-BP20), which we consider to represent the variability of budburst within the



226 population for a given year. BP20 represents the “beginning” of budburst in the tree population, whereas BP80
227 represents its “end.” We chose these quantiles instead of more extreme quantiles of distribution (e.g., 5% and 95%),
228 because they are well represented in our dataset (Fig. 1), thus implying higher model accuracy. For sake of model
229 evaluation, we calculated the DurBB in observed phenology data. Specifically, we selected years which had records
230 before BP20 and after BP80. Then the date of BP20 or BP80 were calculated by using the nearest two data (one is
231 below BP20 or BP80, another is above BP20 or BP80) through interpolation (e.g., 15 % budburst percent is on DoY
232 80 and 25 % budburst percent is on DoY 84. We can obtain the date of BP20 by interpolation, that is DoY 82).

233 **2.8 Statistical analyses**

234 For each population, we quantified by linear regression the sensitivity of budburst date (BP20 and BP80) and the
235 DurBB to time (days year⁻¹) and to Jan-May temperature (days °C⁻¹). Analysis of Variance (ANOVA) was used to
236 analysis whether the significance of the regression slopes ($\alpha=0.05$). All simulations and statistical analyses were
237 carried out with R statistical software v.4.0.3 (R Development Core Team, 2020).



238

239 **Fig. 1. Observed percentage of budburst in five tree populations during the period 2000-2022. The size of the points is scaled**
 240 **with the square root of the number of trees observed. The lines connect the dates of the same year.**

241 **3. Results**

242 **3.1 Phenological observations**

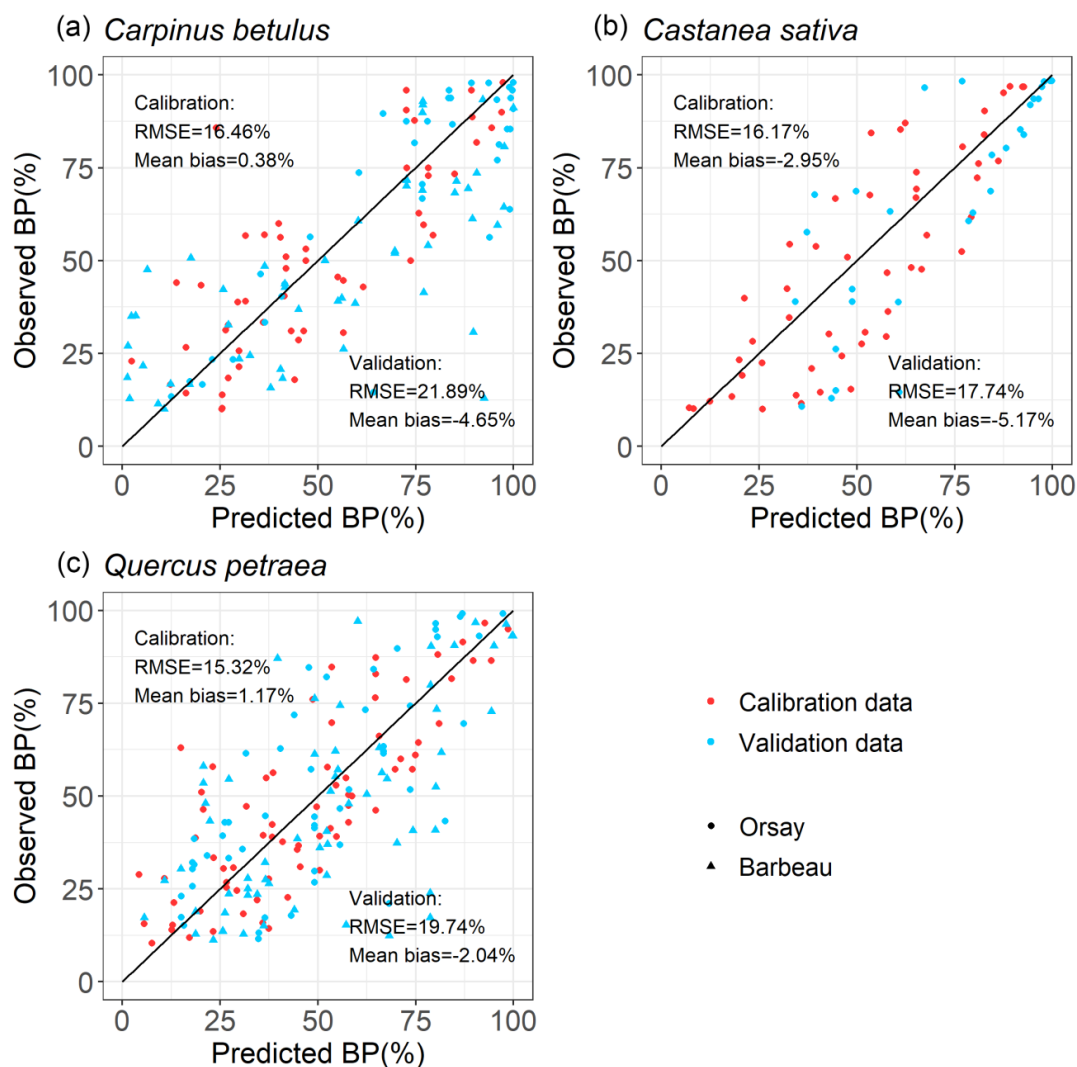
243 Figure 1 shows the observed percentages of budburst in the five tree populations monitored from 2000 to 2022. These
 244 percentage data were established based on 48,442 observations of budburst collected from individual trees. Among the
 245 species, hornbeam was the earliest to reach budburst, typically over DoY 70-100, followed by oak over DoY 90-110,
 246 and finally, chestnut over DoY 100-130. The budburst dates of the oak and hornbeam populations at Barbeau and



247 Orsay were very close, with average differences of 2 and 1 days (Table S1). The duration of budburst in the population
248 (DurBB) (i.e., time interval, in days, during which the proportion of trees having reached budburst increases from 20%
249 to 80%) differs for each species depending on the site and year, with a mean of 8 days over the whole dataset and
250 ranging from 3 days for hornbeam at Orsay in 2018 and 2021 to 21 days for oak at Orsay in 2012 (Fig.1).

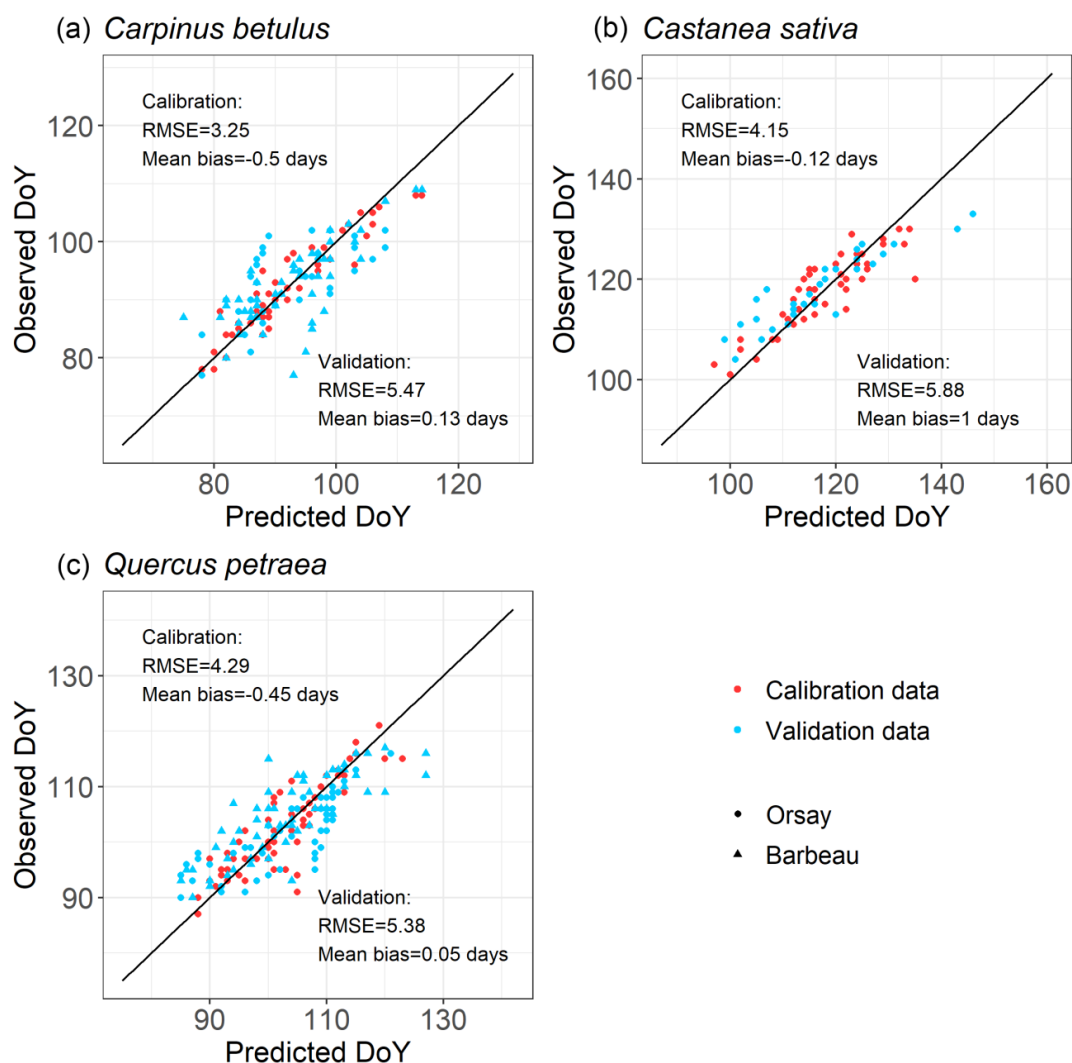
251 **3.2 Model performance**

252 For all the populations considered here, the WPV model predicted with good accuracy the progress of budburst in tree
253 populations during spring as well as the interannual variability of budburst (Fig. 2, Fig. 3; see Fig. S4 for a comparison
254 of observed and simulated time series). The model predicted the percentage of budburst in tree populations with an
255 error ($RMSE_{BP}$) of $16\% \pm 0.2\%$ for the calibration dataset and $20\% \pm 2.1\%$ for the validation dataset. This corresponded
256 to prediction errors for the date of budburst ($RMSE_{DOY}$) of 3.9 ± 0.6 days for the calibration dataset and 5.6 ± 0.3 days
257 for the validation dataset. This compared well to the time resolution of the phenological observations (3-7 days). The
258 mean bias was within 1 day (Fig. 3).



259

260 Fig. 2. Evaluation of the within-population variability (WPV) model predicting the budburst percentage over calibration
 261 (red points) and validation (blue points) data. The points of circle are observed in Orsay and of triangle are observed in
 262 Barbeau. The points establish the correspondence between the observed and predicted percentage of budburst on an
 263 observation day in the population of interest. The one-to-one relation is shown as the black line. RMSE which is root mean
 264 square error for the budburst percentage and mean bias are shown. There are 52, 71 and 50 points (i.e., observation dates)
 265 for calibration and 89, 114, 29 points for validation for hornbeam, oak and chestnut, respectively.



266

267 **Fig. 3. Evaluation of the within-population variability (WPV) model predicting budburst dates over calibration (red points)**
 268 **and validation (blue points) data. The points of circle are observed in Orsay and of triangle are observed in Barbeau. The**
 269 **points establish the correspondence between the observed and predicted budburst date on one observation day in the**
 270 **population of interest. The one-to-one relation is shown as the black line. RMSE which is root mean square error for the**
 271 **budburst percentage and mean bias are shown. There are 52, 71 and 50 points (i.e., observation dates) for calibration and**
 272 **89, 114, 29 points for validation for hornbeam, oak and chestnut, respectively.**

273 **3.3 Parameter variations across species**

274 As mentioned earlier, we assumed that the forcing requirement (F^*) followed a normal distribution. The calibration
 275 procedure yielded a set of distribution curves that differed across species (Fig. 4). We observed that the distribution of



276 F^* had a highest mean and standard deviation for oak compared with hornbeam and chestnut (Fig. 4, Table 2). The
 277 distributions of F^* compared well to the actual distribution of forcing accumulation established from observations (Fig.
 278 5b, e, h), validating the choice of the normal distribution. However, the modelled distribution did not overlap exactly
 279 the distribution established from observed data, because the distribution of observations along the BP scale was uneven
 280 (Fig. 5c, f, i). The temperature threshold for chilling accumulation (T_c) ranged from 9.7°C for chestnut to 10.5°C for
 281 hornbeam and oak (Table 2). The temperature threshold for forcing accumulation (T_f) ranged from 3.9°C for hornbeam
 282 to 7.7°C for chestnut (Table 2, Fig. S2). In all species, buds could not begin ontogenetic growth until the accumulation
 283 of chilling to a certain extent (i.e., parameter h was negative for all populations, Table 2). We found that the threshold
 284 of chilling accumulation necessary for the onset of forcing accumulation (i.e., value of $Sr(t)$ from which Co becomes
 285 positive) was very high for early species and decreased for late species (e.g., value of h increased approximately from
 286 -0.98 in hornbeam to 0 in chestnut; see Table 2 and Fig. S2). Prevailing temperatures could compensate for the lack of
 287 chilling accumulation (positive parameter g ; Table 2) in hornbeam and oak, but not in chestnut ($g=0$).

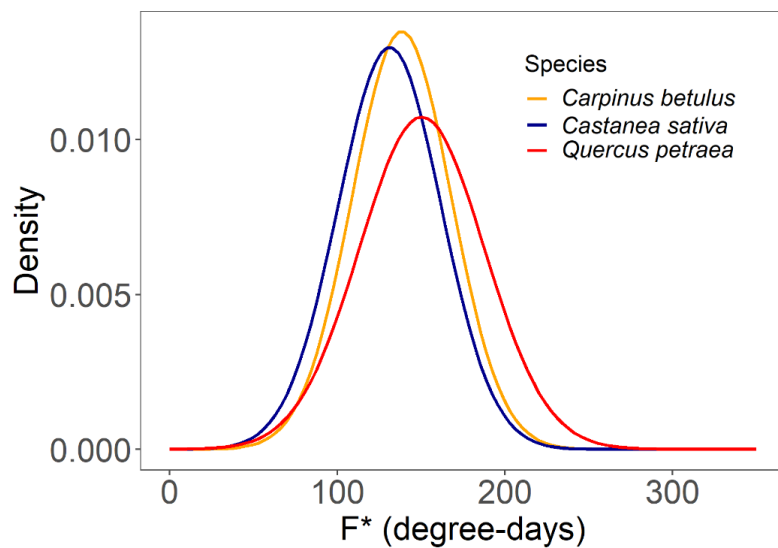
288

289 **Table 2. Parameter values of the WPV model for three populations. μ (°C-days) and σ (°C-days) are the mean and standard**
 290 **deviation of the distribution of F^* , respectively (Eqn. 1). T_b and T_c (°C) are the threshold temperatures for the accumulation**
 291 **of forcing and chilling temperatures, respectively (Eqns. 5 and 9). g (°C⁻¹) and h (dimensionless) are the parameters**
 292 **determining the interactive effect of the state of rest break and the prevailing air temperature on the ontogenetic competence**
 293 **(Eqn. 6). C_{cri} (number of days) is the chilling requirement of rest completion.**

Species	Site	μ	σ	T_b	T_c	g	h	C_{cri}
<i>Carpinus</i>	Orsay	138.4	29.6	3.9	10.5	0.0080	-0.98	155.5
<i>Quercus</i>	Orsay	150.4	37.2	5.3	10.5	0.0032	-0.89	153.0
<i>Castanea</i>	Orsay	131.2	30.7	7.7	9.7	0.0000	-0.02	144.9

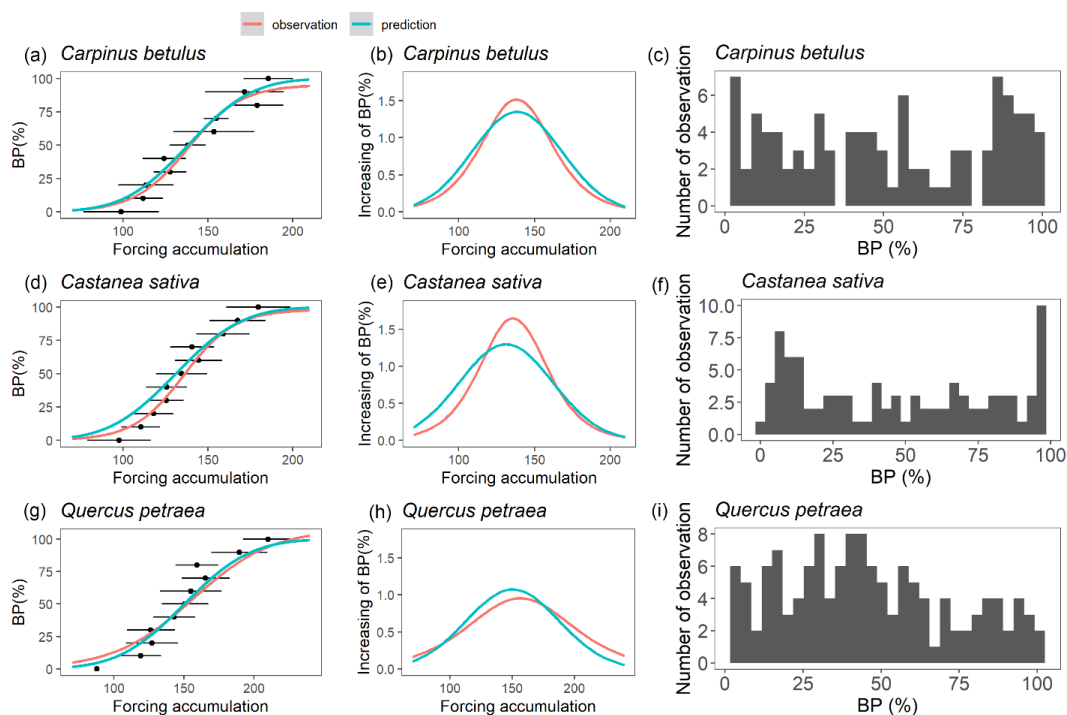
294

295



296

297 **Fig. 4. Normal distribution of the forcing requirement (F^*) for three tree species.**



298

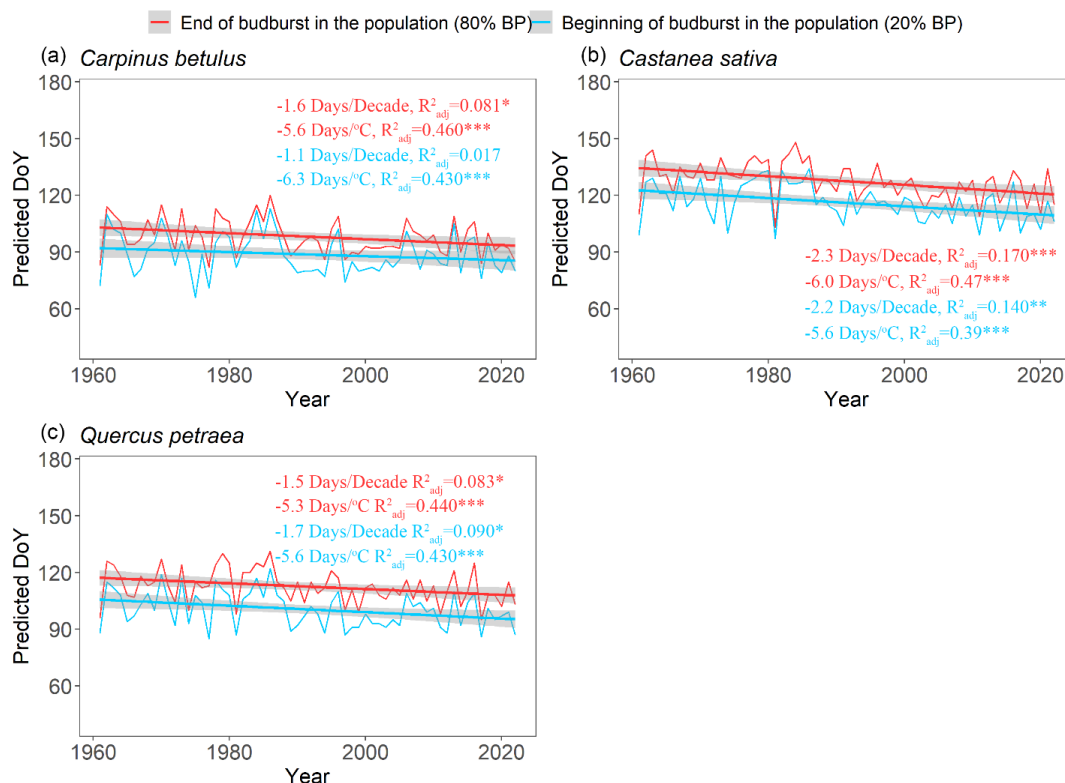
299 **Fig. 5. Evaluating the modelled F^* distributions. Subplots (a, d and g) represent the relation between budburst percentage**
 300 **(BP) and forcing accumulation. The black points and error bars represent the forcing accumulation required to reach a**



301 given budburst percentage in observed data (average across years \pm one standard deviation). The red curves represent a
 302 sigmoid function fitted to the black dots (a, d, g), and its first derivative (b, e, h). The blue curve represents predictions based
 303 on the parameters in Table 2. Subplots (b, e and h) represent the increasing of BP per unit of forcing accumulation. Subplots
 304 (c, f and i) show the distribution of observed data points in the budburst dataset.

305 3.4 Retrospective analysis for within-population variability of budburst

306 Over the past six decades (1961-2022), spring average temperature increased by $+1.9^{\circ}\text{C}$ in Orsay and $+1.4^{\circ}\text{C}$ in
 307 Barbeau (Fig. S5). Over this time period, our retrospective simulations suggest that the beginning (20%, BP20) and
 308 end (80%, BP80) of budburst in tree populations has advanced significantly for all the species (Fig. 6), with
 309 respectively 1.7 ± 0.6 days decade $^{-1}$ (mean \pm SD across species) and 1.8 ± 0.4 days decade $^{-1}$ and apparent temperature
 310 sensitivities of 5.8 ± 0.4 days $^{\circ}\text{C}^{-1}$ and 5.6 ± 0.4 days $^{\circ}\text{C}^{-1}$. These similar trends regarding the beginning and end of
 311 budburst result in an unchanged duration of the budburst period (DurBB in the considered populations over the past
 312 62 years (no trend in DurBB is significantly different from zero in Fig. 7, $P>0.05$). Notably, the interannual variability
 313 of DurBB was large (Fig.6), and fairly simulated by our model (RMSE of 3.4 ± 1.8 days).

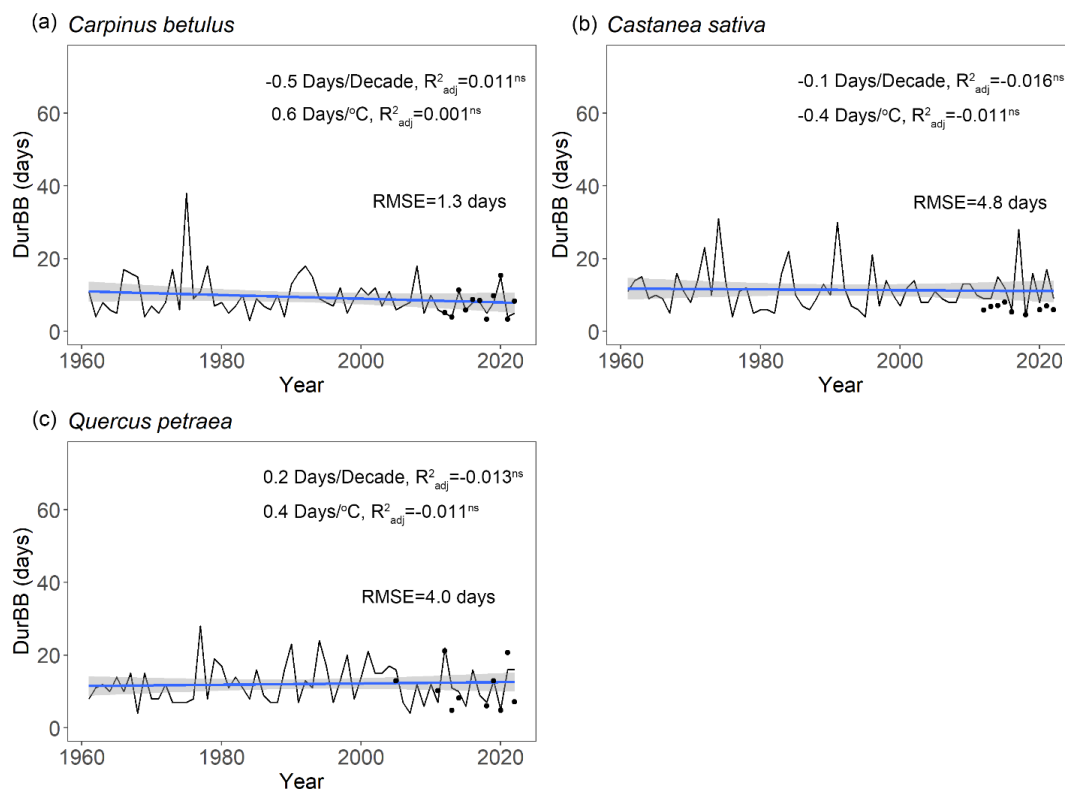


314

315 Fig. 6. Simulated occurrence of the beginning (20%, BP20 in blue) and end (80%, BP80 in red) of budburst using the WPV
 316 model for three tree species during the period 1961-2022. The fitted lines highlight the trends over the past 62 years. Text
 317 in blue (red) shows the sensitivity of BP20 (BP80) to time and mean spring temperature (from January to May), respectively.



318 The sensitivity values are tested by linear regression analyses (*: $P < 0.05$, **: $P < 0.01$, ***: $P < 0.001$) and adjusted coefficient
 319 of determination (R^2_{adj}) is shown.



320

321 **Fig. 7. Simulated duration of budburst in the population (DurBB) using the WPV model for three tree species during the**
 322 **period 1961-2022. The fitted line depicts the change in DurBB over the past 62 years. The sensitivity of DurBB to time and**
 323 **mean spring temperature (from January to May) are tested by linear regression analyses (ns: $P > 0.05$) and adjusted**
 324 **coefficient of determination (R^2_{adj}) is shown. The black points are the actual durations of budburst observed in the data**
 325 **(i.e., restricted to years when both BP20 and BP80 are available in a population).**

326 4. Discussion

327 To the best of our knowledge, this paper presents the first model simulating the within-population variability of
 328 budburst in tree populations. An added value of this model is that it can simulate the duration of budburst in tree
 329 populations. The central hypothesis of the model is that F^* , the amount of accumulated forcing temperature required
 330 for trees to budburst, follows a normal distribution in tree populations. The ability of the model to simulate the
 331 dynamics of budburst over the calibration and validation data, as well as the good agreement between the observed
 332 and the simulated F^* distributions (Fig. 5), lend support to this hypothesis for all the species and populations considered.
 333 Our model yielded RMSE for the validation data (5.4 to 5.9 days), which are close to the temporal resolution of the



334 spring phenology observation (from 2-7 days) and similar to the typical prediction accuracy of models simulating
335 discrete (i.e., population average) budburst dates (e.g., Basler, 2016).

336 The variability in the timing of budburst among individuals in tree populations is considered to be mainly determined
337 by genetic diversity (Bontemps et al., 2016; Delpierre et al., 2017; Jarvinen et al., 2003; Rousi and Heinonen, 2007;
338 Rusanen et al., 2003) followed by the influence of the microenvironment (Delpierre et al., 2017; Rousi and Heinonen,
339 2007). The phenological ranking of individuals is largely conserved in tree populations (Delpierre et al., 2017), leading
340 to the identification of “early,” “intermediate,” and “late” trees (Malyshev et al., 2022). Further, the distribution of
341 budburst categories is not uniform in natural tree populations, with numerous “intermediate” individuals and
342 comparatively fewer “early” and “late” trees (Malyshev et al., 2022; Chesnoiu et al., 2009; Zohner et al., 2018;
343 Caradonna et al., 2014), which lends further support to a unimodal distribution such as the normal law. Our model
344 reproduces this phenomenon, with categories of “early,” “intermediate,” and “late” trees corresponding to increasing
345 values of F^* . This core assumption of the model is supported by previous empirical studies, which observe that the
346 variability of F^* could represent the variability of budburst among trees (Langvall et al., 2001; Rousi and Heinonen,
347 2007). Nevertheless, we could have chosen to assign the variance among individuals to one or several other parameters
348 of the model, related to the fact that genetic variations may affect any of the plant traits determining the modelled
349 parameters. For instance, Gauzere et al. (2019) found that the temperature yielding mid-forcing during ecodormancy
350 (T_{50}) was more sensitive than F^* in the UniChill model, which suggests that this parameter is another good candidate
351 for identifying the phenological behavior of individual trees in a population. Thus, we constructed a model assuming
352 that the threshold for forcing temperature (T_b , i.e., parameter of our model analogous to T_{50}) followed a normal
353 distribution, whereas F^* was fitted as a constant parameter for the population. This model fitted the data less effectively
354 in both the calibration and validation steps (see Fig. S6 and S7 compared with Fig. 2 and 3), which further supports
355 our decision to assign the among-individual variance to F^* . Questions remain regarding the actual shape of the F^*
356 distribution. Indeed, natural selection can lead to traits that are not normally distributed (Caradonna et al., 2014), and
357 uneven distribution of observations may contribute to the non-perfect overlapping of observed and simulated F^*
358 distributions (Fig. 5). However, earlier results (Vallet, 2020) showed that the form of the distribution had little influence
359 on the prediction accuracy.

360 We built the WPV model based on a two-phase parallel model framework, which describes the cumulative effect of
361 chilling and forcing temperatures on the endodormancy and ecodormancy phases, respectively (Hänninen, 2016;
362 Hänninen and Kramer, 2007; Lundell et al., 2020; Chuine and Regniere, 2017). This model structure is in line with
363 our current understanding of the physiological and molecular basis of dormancy in which the dynamics of the
364 dormancy mechanism are emphasized as opposed to a strict classification between the dormancy stages (Lundell et al.,
365 2020; Cooke et al., 2012). In this study, the threshold of chilling accumulation is up to 10.5°C for oak and hornbeam.
366 It is consistent with the experimental results in Baumgarten et al. (2021) which challenge the common assumption that
367 optimal chilling temperatures range ca. 4–6°C, showing 10°C is also effective for chilling accumulation in six dominant
368 temperate European tree species including oak. Furthermore, the model uses the concept of ontogenetic competence
369 (Co) to simulate the process of regulation for the rate of ontogenetic growth by the state of rest break, a phenomenon
370 that has found support in phenological experiments (Lundell et al., 2020; Zhang et al., 2022). Our results demonstrate



371 that in the investigated species, Co is 0 until dormancy is released to a certain extent (Fig. S2), that is, ontogenetic
372 growth cannot start before a certain amount of chilling accumulation has been reached, which is consistent with
373 previous findings (Lundell et al., 2020; Zhang et al., 2022). According to the calibrated parameter values, ontogenetic
374 competence is also influenced by the prevailing temperature, although the effect is minimal. Indeed, parameter g ,
375 which is related to the effect of the prevailing temperature, ranges from 0 to 0.0080 (Table 2), which is comparable to
376 values found in a previous study (Lundell et al., 2020). To some extent in this model, one consequence is that the effect
377 of the prevailing temperature can compensate for the deficiency of chilling accumulation.

378 Beyond introducing a model to describe the WPV of budburst in tree populations, our study aimed to quantify the
379 response of the duration of budburst (DurBB) to climate warming. We used temperature data to simulate the occurrence
380 of 20% (BP20) and 80% (BP80) budburst, and DurBB over the past decades. Our results suggest that the start and end
381 of budburst in tree populations have advanced over the past 62 years with climate warming (Fig. 6), which is consistent
382 with previous results showing advances in the population average dates of budburst (Wenden et al., 2020; Menzel et
383 al., 2006; Fu et al., 2015). In addition, our model simulates sensitivities of budburst to time and temperature that are
384 comparable to values reported earlier (Vitasse et al., 2009b, see Table S2). Our results point to significant sensitivities
385 to both time and temperature for oak as well as significant sensitivity to temperature for hornbeam, which is consistent
386 with the results of Vitasse et al. (2009b).

387 Our retrospective simulations suggest that there was not trend in the duration of budburst in tree populations, DurBB,
388 over the past 62 years (Fig. 7), in spite of climate warming (Fig. S5). Since both BP20 and BP80 advanced at a similar
389 rate, DurBB did not evolve over time over the 1961-2022 period. Interestingly, the analysis of temperature data
390 revealed no significant warming in the period of time from BP20 to BP80 over the past decades ($P > 0.05$, Fig. S8). This
391 could explain why DurBB (time interval between BP20 and BP80) did not change over time, in spite of the strong
392 trends in both BP20 and BP80, caused by climate warming. Moreover, our study sites are located in the temperate
393 zone, at the heart (for oak and hornbeam) and at the north (chestnut) of our study species distribution areas (Caudullo
394 et al., 2017). At those sites, trees can accumulate enough chilling, or at least, chilling accumulation is not a limitation
395 for ontogenetic growth in nature so far, meaning that budburst is still advancing (Wenden et al., 2020; Piao et al., 2019).
396 Thus, the phenomenon by which DurBB increased with insufficient chilling accumulation in a given population (see
397 Zhang et al., 2021), their Fig. 2, 3, 4 for evidence in subtropical trees) did not appear in our retrospective simulations.
398 However, we can infer that if chilling accumulation can't be fulfilled under future, continuous climate warming, it will
399 take more time to fulfill the forcing requirement for late trees with a high forcing requirement, leading to the prolonging
400 of DurBB. A longer duration of budburst would increase the possibility of damage (i.e., freezing, insect damage).
401 These results suggest that the WPV of budburst should be given greater attention, because the longer duration of
402 budburst may be an important factor in the future when researchers project the damage in forests or determine the best
403 strategy for forest management.

404 We acknowledge that the projections of the WPV of budburst produced by the model are uncertain, first and foremost
405 because the parameter values were inferred from observation data collected in natural conditions as opposed to
406 controlled experiments (Hanninen et al., 2019). Another cause of uncertainty is the ability of the phenological response



407 of plants to acclimatize to the changing climate (Bennie et al., 2010). Under the hypothesis of plant acclimatization,
408 the parameters of the WPV model could have changed over the past decades, and would further change with ongoing
409 climate warming. Consequently, related experiments are urgently needed to improve our understanding of the WPV
410 of budburst to infer more reliable parameters and analyze the behavior of phenology models in different climates
411 (Hanninen et al., 2019). However, because our model addresses for the first time explicitly the within-population
412 variation of the physiological traits affecting phenology, it can contribute as a framework for future experimental
413 studies. In our study, we only considered the effect of temperature on budburst. However, other environmental factors
414 may also affect budburst (e.g., photoperiod). Previous studies showed that photoperiod is expected to modulate the
415 timing of budburst in late-successional species such as oak and chestnut, but not in early-successional species such as
416 hornbeam (Basler and Korner, 2012), but see a counter-example on oak in Malyshev et al. (2018). Moreover,
417 photoperiod may have a more complex interaction mechanism with temperature in terms of regulating the time of
418 budburst (Meng et al., 2021). We envision that improved versions of the WPV of budburst could be proposed based
419 on a more comprehensive understanding of the potential mechanism between phenology and environmental factors in
420 the future.

421 **5. Conclusion**

422 In conclusion, our work presents a novel model, simulating the continuity of budburst in tree populations in spring.
423 This phenological model can be adapted to the study of other stages of the tree phenological cycle, which are all of
424 continuous nature in tree populations (e.g., leaf senescence, wood formation etc.). We found budburst was advanced
425 in the past 62 years due to climate warming. However, the duration of budburst period of population was not affected
426 by increasing temperature. This is the first model simulating the within population variability of budburst in the
427 population. It provides a basis for implementation of a module in models directly interested in the within-population
428 variability of phenological and other functional traits (e.g., physio-demo-genetic models). It can also be used as a stand-
429 alone, to study the dynamics of phenological traits from the scale of individuals to the population and community in
430 the context of climate change.

431 **Code and data availability**

432 The related phenology data and R code for the phenological model are openly accessible under
433 <https://doi.org/10.5281/zenodo.7962840> and <https://doi.org/10.5281/zenodo.7188160>, respectively.

434 **Authors' contributions**

435 ND and JL designed the research. ND, JL, AM, GV, DB collected phenological data. JL and ND performed the
436 research. JL wrote the manuscript with substantial inputs from all co-authors.

437 **Competing interests**

438 The authors declare that they have no conflict of interest.



439 **Acknowledgements**

440 We acknowledge Eric Dufrêne for setting up the phenological surveys. We are also grateful to Eric Dufrêne and Jean-
441 Yves Pontailler for their invaluable contributions regarding the collection of phenological data. This work was
442 supported by the China Scholarship Council (202008330320).

443 **References**

- 444 Alberto, F., Bouffier, L., Louvet, J. M., Lamy, J. B., Delzon, S., and Kremer, A.: Adaptive responses for seed and
445 leaf phenology in natural populations of sessile oak along an altitudinal gradient, *J Evol Biol*, 24, 1442-1454,
446 10.1111/j.1420-9101.2011.02277.x, 2011.
- 447 Basler, D.: Evaluating phenological models for the prediction of leaf-out dates in six temperate tree species across
448 central Europe, *Agricultural and Forest Meteorology*, 217, 10-21, 10.1016/j.agrformet.2015.11.007, 2016.
- 449 Basler, D. and Korner, C.: Photoperiod sensitivity of bud burst in 14 temperate forest tree species, *Agricultural and*
450 *Forest Meteorology*, 165, 73-81, 10.1016/j.agrformet.2012.06.001, 2012.
- 451 Baumgarten, F., Zohner, C. M., Gessler, A., and Vitasse, Y.: Chilled to be forced: the best dose to wake up buds
452 from winter dormancy, *New Phytol*, 230, 1366-1377, 10.1111/nph.17270, 2021.
- 453 Bennie, J., Kubin, E., Wiltshire, A., Huntley, B., and Baxter, R.: Predicting spatial and temporal patterns of bud-burst
454 and spring frost risk in north-west Europe: the implications of local adaptation to climate, *Global Change Biology*,
455 16, 1503-1514, 10.1111/j.1365-2486.2009.02095.x, 2010.
- 456 Blanquart, F., Kaltz, O., Nuismer, S. L., and Gandon, S.: A practical guide to measuring local adaptation, *Ecol Lett*,
457 16, 1195-1205, 10.1111/ele.12150, 2013.
- 458 Bontemps, A., Lefevre, F., Davi, H., and Oddou-Muratorio, S.: In situ marker-based assessment of leaf trait
459 evolutionary potential in a marginal European beech population, *J Evol Biol*, 29, 514-527, 10.1111/jeb.12801, 2016.
- 460 CaraDonna, P. J., Iler, A. M., and Inouye, D. W.: Shifts in flowering phenology reshape a subalpine plant
461 community, *Proc Natl Acad Sci U S A*, 111, 4916-4921, 10.1073/pnas.1323073111, 2014.
- 462 Caudullo, G., Welk, E., and San-Miguel-Ayanz, J.: Chorological maps for the main European woody species, *Data*
463 *Brief*, 12, 662-666, 10.1016/j.dib.2017.05.007, 2017.
- 464 Chen, L., Huang, J. G., Ma, Q., Hanninen, H., Tremblay, F., and Bergeron, Y.: Long-term changes in the impacts of
465 global warming on leaf phenology of four temperate tree species, *Global Change Biology*, 25, 997-1004,
466 10.1111/gcb.14496, 2019.
- 467 Chen, L., Huang, J. G., Ma, Q., Hanninen, H., Rossi, S., Piao, S., and Bergeron, Y.: Spring phenology at different
468 altitudes is becoming more uniform under global warming in Europe, *Global Change Biology*, 24, 3969-3975,
469 10.1111/gcb.14288, 2018.



- 470 Chen, X. Q., Wang, L. X., and Inouye, D.: Delayed response of spring phenology to global warming in subtropics
471 and tropics, *Agricultural and Forest Meteorology*, 234, 222-235, 10.1016/j.agrformet.2017.01.002, 2017.
- 472 Chesnoiu, E. N., Șofletea, N., Curtu, A. L., Toader, A., Radu, R., and Enescu, M.: Bud burst and flowering
473 phenology in a mixed oak forest from Eastern Romania, *Annals of Forest Research*, 52, 199-206,
474 doi:10.15287/afr.2009.136, 2009.
- 475 Chuine, I. and Regnier, J.: Process-Based Models of Phenology for Plants and Animals, *Annual Review of Ecology,*
476 *Evolution, and Systematics*, 48, 159-182, 10.1146/annurev-ecolsys-110316-022706, 2017.
- 477 Cooke, J. E., Eriksson, M. E., and Junttila, O.: The dynamic nature of bud dormancy in trees: environmental control
478 and molecular mechanisms, *Plant Cell Environ*, 35, 1707-1728, 10.1111/j.1365-3040.2012.02552.x, 2012.
- 479 Dantec, C. F., Ducasse, H., Capdevielle, X., Fabreguettes, O., Delzon, S., and Desprez-Loustau, M. L.: Escape of
480 spring frost and disease through phenological variations in oak populations along elevation gradients, *Journal of*
481 *Ecology*, 103, 1044-1056, 10.1111/1365-2745.12403, 2015.
- 482 Delpierre, N., Guillemot, J., Dufrene, E., Cecchini, S., and Nicolas, M.: Tree phenological ranks repeat from year to
483 year and correlate with growth in temperate deciduous forests, *Agricultural and Forest Meteorology*, 234, 1-10,
484 10.1016/j.agrformet.2016.12.008, 2017.
- 485 Delpierre, N., Dufrene, E., Soudani, K., Ulrich, E., Cecchini, S., Boe, J., and Francois, C.: Modelling interannual and
486 spatial variability of leaf senescence for three deciduous tree species in France, *Agricultural and Forest Meteorology*,
487 149, 938-948, 10.1016/j.agrformet.2008.11.014, 2009.
- 488 Delpierre, N., Vitasse, Y., Chuine, I., Guillemot, J., Bazot, S., Rutishauser, T., and Rathgeber, C. B. K.: Temperate
489 and boreal forest tree phenology: from organ-scale processes to terrestrial ecosystem models, *Annals of Forest*
490 *Science*, 73, 5-25, 10.1007/s13595-015-0477-6, 2016.
- 491 Denechere, R., Delpierre, N., Apostol, E. N., Berveiller, D., Bonne, F., Cole, E., Delzon, S., Dufrene, E., Gressler,
492 E., Jean, F., Lebourgeois, F., Liu, G., Louvet, J. M., Parmentier, J., Soudani, K., and Vincent, G.: The within-
493 population variability of leaf spring and autumn phenology is influenced by temperature in temperate deciduous
494 trees, *Int J Biometeorol*, 65, 369-379, 10.1007/s00484-019-01762-6, 2021.
- 495 Du, Y. J., Pan, Y. Q., and Ma, K. P.: Moderate chilling requirement controls budburst for subtropical species in
496 China, *Agricultural and Forest Meteorology*, 278, 107693, ARTN 107693, 10.1016/j.agrformet.2019.107693, 2019.
- 497 Fu, Y. H., Zhang, X., Piao, S., Hao, F., Geng, X., Vitasse, Y., Zohner, C., Penuelas, J., and Janssens, I. A.: Daylength
498 helps temperate deciduous trees to leaf-out at the optimal time, *Global Change Biology*, 25, 2410-2418,
499 10.1111/gcb.14633, 2019.



- 500 Fu, Y. H., Zhao, H., Piao, S., Peaucelle, M., Peng, S., Zhou, G., Ciais, P., Huang, M., Menzel, A., Penuelas, J., Song,
501 Y., Vitasse, Y., Zeng, Z., and Janssens, I. A.: Declining global warming effects on the phenology of spring leaf
502 unfolding, *Nature*, 526, 104-107, 10.1038/nature15402, 2015.
- 503 Gauzere, J., Lucas, C., Ronce, O., Davi, H., and Chuine, I.: Sensitivity analysis of tree phenology models reveals
504 increasing sensitivity of their predictions to winter chilling temperature and photoperiod with warming climate,
505 *Ecological Modelling*, 411, ARTN 108805, 10.1016/j.ecolmodel.2019.108805, 2019.
- 506 Hanninen, H., Kramer, K., Tanino, K., Zhang, R., Wu, J., and Fu, Y. H.: Experiments Are Necessary in Process-
507 Based Tree Phenology Modelling, *Trends Plant Sci*, 24, 199-209, 10.1016/j.tplants.2018.11.006, 2019.
- 508 Hänninen, H.: Modelling bud dormancy release in trees from cool and temperate regions, *Acta Forestalia Fennica*,
509 10.14214/aff.7660, 1990.
- 510 Hänninen, H.: Boreal and temperate trees in a changing climate: Modelling the ecophysiology of seasonality,
511 Dordrecht: Springer Science +Business Media, 2016.
- 512 Hänninen, H. and Kramer, K.: A framework for modelling the annual cycle of trees in boreal and temperate regions,
513 *Silva Fennica*, 41, 167-205, 2007.
- 514 Hart, S. P., Schreiber, S. J., and Levine, J. M.: How variation between individuals affects species coexistence, *Ecol*
515 *Lett*, 19, 825-838, 10.1111/ele.12618, 2016.
- 516 Jarvinen, P., Lemmetyinen, J., Savolainen, O., and Sapanen, T.: DNA sequence variation in BpMADS2 gene in two
517 populations of *Betula pendula*, *Mol Ecol*, 12, 369-384, 10.1046/j.1365-294x.2003.01740.x, 2003.
- 518 Jewaria, P. K., Hanninen, H., Li, X., Bhalerao, R. P., and Zhang, R.: A hundred years after: endodormancy and the
519 chilling requirement in subtropical trees, *New Phytol*, 231, 565-570, 10.1111/nph.17382, 2021.
- 520 Kramer, K.: A Modeling Analysis of the Effects of Climatic Warming on the Probability of Spring Frost Damage To
521 Tree Species in the Netherlands and Germany, *Plant Cell Environ*, 17, 367-377, 10.1111/j.1365-
522 3040.1994.tb00305.x, 1994.
- 523 Kramer, K., Buiteveld, J., Forstreuter, M., Geburek, T., Leonardi, S., Menozzi, P., Povillon, F., Schelhaas, M., du
524 Cros, E. T., Vendramin, G. G., and van der Werf, D. C.: Bridging the gap between ecophysiological and genetic
525 knowledge to assess the adaptive potential of European beech, *Ecological Modelling*, 216, 333-353,
526 10.1016/j.ecolmodel.2008.05.004, 2008.
- 527 Langvall, O., Nilsson, U., and Orlander, G.: Frost damage to planted Norway spruce seedlings - influence of site
528 preparation and seedling type, *Forest Ecology and Management*, 141, 223-235, 10.1016/S0378-1127(00)00331-5,
529 2001.



- 530 Liu, G. H., Chuine, I., Denechere, R., Jean, F., Dufrene, E., Vincent, G., Berveiller, D., and Delpierre, N.: Higher
531 sample sizes and observer inter-calibration are needed for reliable scoring of leaf phenology in trees, *Journal of*
532 *Ecology*, 109, 2461-2474, 10.1111/1365-2745.13656, 2021.
- 533 Lundell, R., Hanninen, H., Saarinen, T., Astrom, H., and Zhang, R.: Beyond rest and quiescence (endodormancy and
534 ecodormancy): A novel model for quantifying plant-environment interaction in bud dormancy release, *Plant Cell*
535 *Environ*, 43, 40-54, 10.1111/pce.13650, 2020.
- 536 Malyshev, A. V., Henry, H. A. L., Bolte, A., Khan, M. A. S. A., and Kreyling, J.: Temporal photoperiod sensitivity
537 and forcing requirements for budburst in temperate tree seedlings, *Agricultural and Forest Meteorology*, 248, 82-90,
538 10.1016/j.agrformet.2017.09.011, 2018.
- 539 Malyshev, A. V., van der Maaten, E., Garthen, A., Mass, D., Schwabe, M., and Kreyling, J.: Inter-Individual
540 Budburst Variation in *Fagus sylvatica* Is Driven by Warming Rate, *Front Plant Sci*, 13, 853521,
541 10.3389/fpls.2022.853521, 2022.
- 542 Meier, U.: Growth stages of mono-and dicotyledonous plants., *BBCH Monograph*, Blackwell Wissenschafts-Verlag
543 Berlin Wien, 1997.
- 544 Meng, L., Zhou, Y., Gu, L., Richardson, A. D., Penuelas, J., Fu, Y., Wang, Y., Asrar, G. R., De Boeck, H. J., Mao,
545 J., Zhang, Y., and Wang, Z.: Photoperiod decelerates the advance of spring phenology of six deciduous tree species
546 under climate warming, *Global Change Biology*, 27, 2914-2927, 10.1111/gcb.15575, 2021.
- 547 Menzel, A., Sparks, T. H., Estrella, N., Koch, E., Aasa, A., Ahas, R., Alm-Kubler, K., Bissolli, P., Braslavskaja, O.,
548 Briede, A., Chmielewski, F. M., Crepinsek, Z., Curnel, Y., Dahl, A., Defila, C., Donnelly, A., Filella, Y., Jatca, K.,
549 Mage, F., Mestre, A., Nordli, O., Penuelas, J., Pirinen, P., Remisova, V., Scheifinger, H., Striz, M., Susnik, A., Van
550 Vliet, A. J. H., Wielgolaski, F. E., Zach, S., and Zust, A.: European phenological response to climate change matches
551 the warming pattern, *Global Change Biology*, 12, 1969-1976, 10.1111/j.1365-2486.2006.01193.x, 2006.
- 552 Morente-Lopez, J., Kass, J. M., Lara-Romero, C., Serra-Diaz, J. M., Soto-Correa, J. C., Anderson, R. P., and Iriondo,
553 J. M.: Linking ecological niche models and common garden experiments to predict phenotypic differentiation in
554 stressful environments: Assessing the adaptive value of marginal populations in an alpine plant, *Global Change*
555 *Biology*, 28, 4143-4162, 10.1111/gcb.16181, 2022.
- 556 Oddou-Muratorio, S. and Davi, H.: Simulating local adaptation to climate of forest trees with a Physio-Demo-
557 Genetics model, *Evol Appl*, 7, 453-467, 10.1111/eva.12143, 2014.
- 558 Parmesan, C. and Yohe, G.: A globally coherent fingerprint of climate change impacts across natural systems,
559 *Nature*, 421, 37-42, 10.1038/nature01286, 2003.
- 560 Petit, R. J. and Hampe, A.: Some evolutionary consequences of being a tree, *Annual Review of Ecology Evolution*
561 *and Systematics*, 37, 187-214, 10.1146/annurev.ecolsys.37.091305.110215, 2006.



- 562 Piao, S., Liu, Q., Chen, A., Janssens, I. A., Fu, Y., Dai, J., Liu, L., Lian, X., Shen, M., and Zhu, X.: Plant phenology
563 and global climate change: Current progresses and challenges, *Global Change Biology*, 25, 1922-1940,
564 10.1111/gcb.14619, 2019.
- 565 Puchalka, R., Koprowski, M., Przybylak, J., Przybylak, R., and Dabrowski, H. P.: Did the late spring frost in 2007
566 and 2011 affect tree-ring width and earlywood vessel size in Pedunculate oak (*Quercus robur*) in northern Poland?,
567 *Int J Biometeorol*, 60, 1143-1150, 10.1007/s00484-015-1107-6, 2016.
- 568 R Core Team. R: A language and environment for statistical computing. R Foundation for Statistical Computing,
569 Vienna, Austria. URL <https://www.R-project.org/>, 2020
- 570 Rathgeber, C. B., Rossi, S., and Bontemps, J. D.: Cambial activity related to tree size in a mature silver-fir
571 plantation, *Ann Bot*, 108, 429-438, 10.1093/aob/mcr168, 2011.
- 572 Renner, S. S. and Zohner, C. M.: Climate Change and Phenological Mismatch in Trophic Interactions Among Plants,
573 Insects, and Vertebrates, *Annu Rev Ecol Evol S*, 49, 165-182, 10.1146/annurev-ecolsys-110617-062535, 2018.
- 574 Richardson, A. D., Black, T. A., Ciais, P., Delbart, N., Friedl, M. A., Gobron, N., Hollinger, D. Y., Kutsch, W. L.,
575 Longdoz, B., Luysaert, S., Migliavacca, M., Montagnani, L., Munger, J. W., Moors, E., Piao, S., Rebmann, C.,
576 Reichstein, M., Saigusa, N., Tomelleri, E., Vargas, R., and Varlagin, A.: Influence of spring and autumn
577 phenological transitions on forest ecosystem productivity, *Philos Trans R Soc Lond B Biol Sci*, 365, 3227-3246,
578 10.1098/rstb.2010.0102, 2010.
- 579 Rousi, M. and Heinonen, J.: Temperature sum accumulation effects on within-population variation and long-term
580 trends in date of bud burst of European white birch (*Betula pendula*), *Tree Physiol*, 27, 1019-1025,
581 10.1093/treephys/27.7.1019, 2007.
- 582 Rusanen, M., Vakkari, P., and Blom, A.: Genetic structure of *Acer platanoides* and *Betula pendula* in northern
583 Europe, *Can J Forest Res*, 33, 1110-1115, 10.1139/X03-025, 2003.
- 584 Scotti, I., González-Martínez, S. C., Budde, K. B., and Lalagüe, H.: Fifty years of genetic studies: what to make of
585 the large amounts of variation found within populations?, *Annals of Forest Science*, 73, 69-75, 10.1007/s13595-015-
586 0471-z, 2016.
- 587 Vallet, L.: Modélisation de la dynamique intra-populationnelle du débournement en Ile-de-France, MSc report,
588 Université Paris-Saclay, Orsay, France, 2020.
- 589 Vegis, A.: Dormancy in Higher Plants, *Annual Review of Plant Physiology*, 15, 185-+,
590 10.1146/annurev.pp.15.060164.001153, 1964.
- 591 Vidal, J. P., Martin, E., Franchisteguy, L., Baillon, M., and Soubeyroux, J. M.: A 50-year high-resolution
592 atmospheric reanalysis over France with the Safran system, *International Journal of Climatology*, 30, 1627-1644,
593 10.1002/joc.2003, 2010.



- 594 Violle, C., Enquist, B. J., McGill, B. J., Jiang, L., Albert, C. H., Hulshof, C., Jung, V., and Messier, J.: The return of
595 the variance: intraspecific variability in community ecology, *Trends Ecol Evol*, 27, 244-252,
596 10.1016/j.tree.2011.11.014, 2012.
- 597 Vitasse, Y. and Basler, D.: What role for photoperiod in the bud burst phenology of European beech, *European*
598 *Journal of Forest Research*, 132, 1-8, 10.1007/s10342-012-0661-2, 2013.
- 599 Vitasse, Y., Porte, A. J., Kremer, A., Michalet, R., and Delzon, S.: Responses of canopy duration to temperature
600 changes in four temperate tree species: relative contributions of spring and autumn leaf phenology, *Oecologia*, 161,
601 187-198, 10.1007/s00442-009-1363-4, 2009a.
- 602 Vitasse, Y., Delzon, S., Dufrière, E., Pontailleur, J.-Y., Louvet, J.-M., Kremer, A., and Michalet, R.: Leaf phenology
603 sensitivity to temperature in European trees: Do within-species populations exhibit similar responses?, *Agricultural*
604 *and Forest Meteorology*, 149, 735-744, 10.1016/j.agrformet.2008.10.019, 2009b.
- 605 Walther, G. R., Post, E., Convey, P., Menzel, A., Parmesan, C., Beebee, T. J., Fromentin, J. M., Hoegh-Guldberg, O.,
606 and Bairlein, F.: Ecological responses to recent climate change, *Nature*, 416, 389-395, 10.1038/416389a, 2002.
- 607 Wenden, B., Mariadassou, M., Chmielewski, F. M., and Vitasse, Y.: Shifts in the temperature-sensitive periods for
608 spring phenology in European beech and pedunculate oak clones across latitudes and over recent decades, *Global*
609 *Change Biology*, 26, 1808-1819, 10.1111/gcb.14918, 2020.
- 610 Zhang, R., Lin, J. H., Wang, F. C., Delpierre, N., Kramer, K., Hanninen, H., and Wu, J. S.: Spring phenology in
611 subtropical trees: Developing process-based models on an experimental basis, *Agricultural and Forest Meteorology*,
612 314, ARTN 108802, 10.1016/j.agrformet.2021.108802, 2022.
- 613 Zhang, R., Lin, J. H., Wang, F. C., Shen, S. T., Wang, X. B., Rao, Y., Wu, J. S., and Hanninen, H.: The chilling
614 requirement of subtropical trees is fulfilled by high temperatures: A generalized hypothesis for tree endodormancy
615 release and a method for testing it, *Agricultural and Forest Meteorology*, 298, ARTN 108296,
616 10.1016/j.agrformet.2020.108296, 2021.
- 617 Zohner, C. M., Mo, L., and Renner, S. S.: Global warming reduces leaf-out and flowering synchrony among
618 individuals, *Elife*, 7, 10.7554/eLife.40214, 2018.
- 619 Zohner, C. M., Mo, L., Sebald, V., Renner, S. S., and Dornelas, M.: Leaf-out in northern ecotypes of wide-ranging
620 trees requires less spring warming, enhancing the risk of spring frost damage at cold range limits, *Global Ecology*
621 *and Biogeography*, 29, 1065-1072, 10.1111/geb.13088, 2020.

622